Hadron production at the LHC: Any indication of new phenomena

Eugene Levin[1, 2] and Amir H. Rezaeian[2]
[1]*Department of Particle Physics, Tel Aviv University, Tel Aviv 69978, Israel*
[2]*Departamento de Física, Universidad Técnica Federico Santa María,*
Avda. España 1680, Casilla 110-V, Valparaiso, Chile

(Dated: November 17, 2010)

We confront soft Pomeron and gluon saturation models with the first LHC data on inclusive hadron production. We claim that while the first type of models are not able to describe some part of the LHC data, the Colour-Glass-Condensate (gluon saturation) approach gives an adequate description of the data. Here, we compare our published predictions with the recently available 7 TeV data. We firmly believe that if further experimental measurements confirm that the gluon saturation works, it will be a major discovery.

I. INTRODUCTION

As it was expected the first data from the LHC are on soft interaction at high energies such as the total and diffractive cross-sections, the hadron inclusive production and so on. Therefore, it is a proper time to review our understanding of these processes.

For four decades, the main tool for description of soft interaction has been the approach based on Reggeons and Pomerons and their interactions. The first good news is that actually for the first time in these four decades we obtain Pomeron from theory. Today Pomeron is not a plausible assumption as it was in the 70s, it is not the object of successful high energy phenomenology but it comes out naturally from the first theory of strong interaction: N=4 Super Yang Mills (N=4 SYM) [1]. N=4 SYM together with AdS/CFT correspondence allows us to study the regime of the strong coupling constant [2]. For the first time we have a theory which leads to the main ingredients of the high-energy phenomenology such as Pomerons and Reggeons, in the limit of strong coupling. On the other hand, N=4 SYM with small coupling leads to normal QCD like physics [3, 4] with OPE and linear equations for DIS as well as the BFKL equation for the high energy amplitude.

First, we recall that N=4 SYM has a simple solution for the following set of couplings:

$$g_s \;=\; \frac{g^2_{YM}}{4\pi} \;=\; \alpha_{YM} \;=\; \frac{\lambda}{4\pi N_c}; \quad R \;=\; \alpha'^{\frac{1}{2}}\,\lambda^{\frac{1}{4}}; \quad g_s \;\ll\; 1; \;\; \text{but} \;\; \lambda \;\gg\; 1, \tag{1}$$

where R is the radius in AdS_5- metric, N_c denotes the number of colours and α' is the slope of the Reggeons ($\alpha' \approx 1\,\mathrm{GeV}^{-2}$) which is intimately related to the string tension in string theory. The Pomeron which appears in N=4 SYM [1] at large λ, has a intercept and a slope of the trajectory that are equal to

$$\alpha_{I\!P}(0) \;=\; 2 \,-\, \frac{2}{\sqrt{\lambda}} \qquad \alpha'_{I\!P}(0) \;=\; 0, \tag{2}$$

in the limit of $\frac{2}{\sqrt{\lambda}} \ll 1$. In the next section we will discuss the main property of the Pomeron in N=4 SYM. We will introduce available models which incorporate those properties. In the framework of N=4 SYM motivated models for soft high-energy interaction, we will then confront these models with the LHC recent data for the inclusive hadron production. Our main conclusion is: it is premature to claim that *soft* model is unable to describe the LHC data, and we need to have precise values of the cross-sections of diffraction processes in order to claim so. On the same footing, we should improve the Monte Carlo based simulation models in order to include those processes.

In the last section, we consider the high-density QCD picture which provides an alternative description of soft high-energy interaction. We will show that the high-density QCD scenario for inclusive hadron production in proton-proton collisions works and gluon saturation reproduces the LHC data for charged-hadron transverse-momentum and multiplicity distribution in rapidity and energy [5]. We show that high-density QCD [5] predicted 7 TeV data in pp collisions [6]. We firmly believe that if further experiments confirm that the gluon saturation works it will be a major discovery. There exists some ideas how to simulate the CGC state in nucleus collisions but evidence for the formation of the CGC state (gluon saturation) in proton-proton interaction will be a triumph of the high-density QCD. The last section is devoted to our predictions for the LHC both for hadron-hadron (pp) and nucleus-nucleus (AA) collisions [7]. We consider this section as a key part of this manuscript since we believe that comparison with our predictions will provide the first hint toward discovery of the new phase of QCD, the CGC at the LHC.

II. INCLUSIVE HADRON PRODUCTION IN SOFT POMERON MODELS

First, let us summarize what we have learned about soft high-energy interaction during the last four decades. The phenomenology based on the Pomerons and their interactions has been very successful in description of the experimental data. On the other hand all attempts to build a theory of Pomeron and Reggeons and their interactions have failed. As it was already mentioned, at present we have two theoretical guides: high energy scattering in N=4 SYM which gives Pomeron interactions, and matching with perturbative QCD where we can use the BFKL Pomeron calculus to obtain the scattering amplitude. Based on these two guides, one can formulate the basic criteria for such models:

(i) Pomeron $\Delta_{I\!P} \approx 0.3$ and $\alpha'_{I\!P} \approx 0$. The large intercept of the Pomeron follows from N=4 SYM and its value about 0.3 follows from the description of the DIS data [8].

(ii) Large Good-Walker component [9] since in N=4 SYM the main contribution stems from the processes of elastic scattering and diffraction production [1, 10].

(iii) Small Pomeron interaction which is of the order of $2/\sqrt{\lambda} \ll 1$ in N=4 SYM [11].

(iv) Only triple Pomeron vertex is essential to provide a natural matching with perturbative QCD [12].

At the moment we have only four models [13–16] on the market that satisfy these criteria. Unfortunately, the inclusive hadron production was predicted in only one model [13] (see Ref. [17] and Fig. 1).

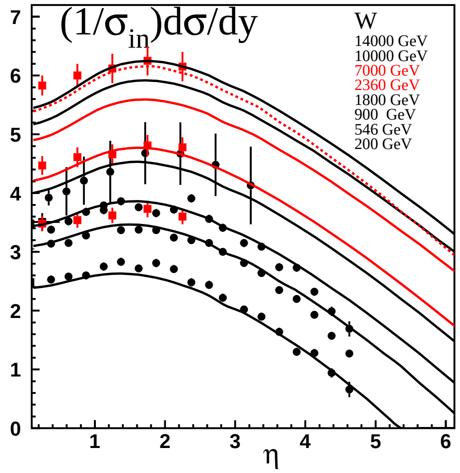

FIG. 1: Hadron multiplicity from the soft Pomeron model [13] at various energy. Dotted curve shows the prediction of Ref. [13] divided by σ_{ND}. The experimental data are from Refs. [6, 18–20].

In Fig. 2, we show the typical Mueller diagrams which is used for the calculation of the inclusive hadron production. In Pomeron type model, we have two main ingredients: the full Pomeron Green function and σ_{in} defined in Fig. 2. It turns out that the main uncertainties stems from the value of σ_{in}. Various predictions for σ_{in} can be extracted from Table I.

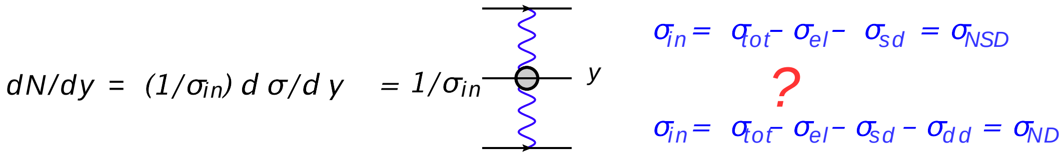

FIG. 2: The Mueller diagram for the inclusive production of hadrons in Pomeron approach. The wave line denotes the full Green function of the Pomeron. σ_{tot}, σ_{el}, σ_{sd} and σ_{dd} denote the total, elastic, single and double diffraction cross-section, respectively.

The curves in Fig. 1 were calculated using $\sigma_{in} = \sigma_{NSD}$. The dotted curve corresponds to $\sigma_{in} = \sigma_{ND}$. One can see that we need to understand better what kind of inclusive production has been measured. The experimental selection of the measured events at the moment apparently depends strongly on the Monte Carlo simulation that has been

	Tevatron (1.8 TeV)					LHC (14 TeV)				
	G(08)	G(10)	K(07)	K(10)	O(C)	G(08)	G(10)	K(07)	K(10)	O(C)
σ_{tot}(mb)	73.29	74.4	74.0	73.9	73.0	92.1	101	88.0	86.3	114.0
σ_{el}(mb)	16.3	17.5	16.3	15.1	16.8	20.9	26.1	20.1	18.1	33.0
σ_{sd}(mb)	9.76	8.87	10.9	12.7	9.6	11.8	10.8	13.3	16.1	11.0
σ_{dd}(mb)	5.36	3.53	7.2	13.3	3.93	6.1	6.5	13.4	12.9	4.83
σ_{NSD}(mb)	47.2	46.9	46.8	43.5	47	61.6	64.1	54.6	51.2	60
σ_{ND}(mb)	41.8	43	41.2		42	50.1	57.6	41.2		56.2

TABLE I: Comparison of various soft models: G(08) denotes the GLMM model [13] in which one sums only enhanced diagrams. G(10) denotes the model of the Tel Aviv group where a general class of the Pomeron diagrams is summed [16]. K(07) and K(10) denote two models of the Durham group. The 2007 predictions are from Ref. [14] and the preliminary 2010 predictions are taken from the talk of A. Martin at Diffraction 2010 workshop. OS(C) is the model developed in Ref. [15].

$\sqrt{s}$ TeV		Pythia6	Phojet	GLMM
0.9	σ_{ND}(mb)	34.4	40.0	39.23
0.9	σ_{sd}(mb)	11.7	10.5	8.24
0.9	σ_{dd}(mb)	6.4	3.5	3.83
7.0	σ_{ND}(mb)	48.5	61.6	51.47
7.0	σ_{sd}(mb)	13.7	10.7	10.2
7.0	σ_{dd}(mb)	9.3	3.9	6.46

TABLE II: Comparison of Monte Carlo simulation models with the GLMM model [13].

used. Table II shows that there is no Monte Carlo code on the market that can consistently describe the diffraction production processes.

Having these two tables in mind, we can conclude that the claim that soft model is not able to describe the LHC data is premature and much more work is needed to prove this claim. However, the LHC recent data includes some interesting measuments such as the dependence of average transverse momentum of produced hadron on energy and multiplicity which cannot be described in framework of Pomeron-type models.

III. HIGH DENSITY QCD AND HADRON PRODUCTION

The conclusion from the previous section is that one has to look for a more adequate approach which provides a better description of the experimental data at the LHC and will be more closely related to QCD.

Fortunately, we have such an approach on the market: high density QCD [21] leads to a completely different picture of inclusive hadron production. In this approach, a system of parton (gluons) at high energy forms a new state of matter: Colour Glass Condensate (CGC). In the CGC picture, at high energy, the density of partons ρ_p with a typical transverse momenta less than Q_s reaches a high value, $\rho_p \propto 1/\alpha_s \gg 1$ (α_s is the strong coupling constant). The saturation scale Q_s is a new momentum scale that increases with energy. At high energies/small Bjorken-x, $Q_s \gg \mu$ where μ is the scale of soft interaction. Therefore, $\alpha_s\left(Q_s\right) \ll 1$ and this fact allows us to treat this system on solid theoretical basis. On the other hand, even though the strong coupling α_S becomes small due to the high density of partons, saturation effects, the fields interact strongly because of the classical coherence. This leads to the a new regime of QCD with non-linear features which cannot be investigated in a more traditional perturbative approach. In the framework of the CGC approach the secondary hadrons are originated from the decay of gluon mini jets with the transverse momentum equal to the saturation scale $Q_s(x)$. The first stage of this process is rather under theoretical control and determines the main characteristics of the hadron production, especially as far as energy, rapidity and transverse momentum dependence are concerned. The jet decay, unfortunately, could be treated mostly phenomenologically.

Actually, such a scenario has passed two critical tests with the experimental data: First, it explains the main features of hadron multiplicity in heavy ion-ion collisions at RHIC (KLN papers [22]); and it gave correct predictions for the inclusive hadron production in proton-proton (pp) collisions [5] at the LHC at $\sqrt{s} = 7$ TeV [6].

The inclusive mini jet cross-section in high-energy pp (or AA) collisions can be calculated within the CGC approach via the k_T factorization [23–25] by convolution of two hadrons (or nucleus) unintegrated gluon distributions

$\phi_G^{h_i(A_i)}(x_i;\vec{k}_T)$, depicted in Fig. 3-a, where $x_{1,2} = (p_T/\sqrt{s})e^{\pm y}$, p_T and y are the transverse-momentum and rapidity of the produced gluon mini jet. The relation between the unintegrated gluon density and the colour dipole-proton (or nucleus) forward scattering amplitude $N_{h_i(A_i)}(x_i;r_T;b)$ was obtained in Ref. [24] which relates the hadron production in pp (or AA) collisions to deep inelastic lepton-hadron scattering (DIS) at small Bjorken-x at HERA. It reads as follows

$$\phi_G^{h_i(A_i)}\left(x_i;\vec{k}_T\right) = \frac{1}{\alpha_s}\frac{N_c^2-1}{2(2\pi)^3N_c}\int d^2\vec{b}d^2\vec{r}_T e^{i\vec{k}_T\cdot\vec{r}_T}\nabla_T^2 N_G^{h_i(A_i)}(x_i;r_T;b)\,, \tag{3}$$

with notation

$$N_G^{h_i(A_i)}(x_i;r_T;b) = 2N_{h_i(A_i)}(x_i;r_T;b) - N^2_{h_i(A_i)}(x_i;r_T;b)\,, \tag{4}$$

where r_T denotes the dipole transverse size and $\vec{b}$ is the impact parameter of the scattering. Notice that the relation between the unintegrated gluon density and the forward dipole amplitude in the k_T factorization is not a simple Fourier transformation which is commonly used in literature and also depends on the impact-parameter. The impact-parameter dependence in these equations is not trivial and should not be in principle assumed as an over-all factor. For the dipole amplitude, we use the b-CGC saturation model [26] which is the generalization of the approach given in Refs. [27, 28] and effectively incorporates all known saturation properties [5] driven by the small-x non-linear evolution equations including the impact-parameter dependence of the dipole amplitude [29]. This model describes both the HERA DIS data at small-x [26], direct-photon production [30] and the inclusive hadron production in pp collisions [5]. The extension of this model for the case of nuclear target was introduced in Ref. [7] which also give a good description of RHIC multiplicity data.

The main contribution of the k_T factorization in the multiplicity comes from $p_T < 2$ GeV. For such a kinematic region at very low-p_T, we rely on the Local Parton-Hadron Duality principle [31], namely we assume that the hadronization is a soft process and cannot change the direction of the emitted radiation. This works perfectly in e^+e^- annihilation into hadrons [31, 32] and we believe that this is more preferable than to deal with the fragmentation functions for which we have no theoretical justifications at low p_T. Hence, the form of the rapidity distribution of the mini jet and the produced hadron Eq. (5) are different only with a numerical factor C, and the transverse momentum of jet and the produced hadron are related with a factor $\langle z\rangle$. In the spirit of the geometrical-scaling property of the scattering amplitude, we obtain the charged-particle multiplicity distribution at a fixed centrality but various energies from the corresponding mini jet cross-section divided by the average area of interaction $\sigma_s \propto \pi\left\langle \vec{b}^2_{jet}\right\rangle$, see Fig. 3-b. The p_T spectrum of the produced hadron can be then related to the cross-section of the mini jet production in the following way:

$$\frac{dN_{\text{hadron}}}{d^2p_T} = C\int d\eta\, h[\eta]\frac{1}{\sigma_s}\,\frac{d\sigma^{\text{mini jet}}}{d\eta\, d^2p_{\text{jet},T}}\left[\text{with } p_{\text{jet},T} = p_T/\langle z\rangle\right]. \tag{5}$$

Notice that k_T factorization has infrared divergence. By introducing a new parameter m_{eff} as mini jet mass which mimics the pre-hadronization effect, one can also regularize the cross-section. Therefore, we have only two unknown parameters in our model, the overall factor C and the mini jet mass m_{jet} which are fixed at lower energy. Then our results at higher energies and rapidities can be considered as free-parameter predictions.

Fig. 3 shows our description of the existing experimental data and predictions for higher energies. In this figure, we show for the first time the comparison of our prediction [5] with 7 TeV pp data [6]. One can see that the agreement is striking. It should be stressed that our approach gives a quite different result for the LHC energies in comparison with the Kharzeev-Levin-Nardi (KLN) approach [22] both for pp and AA collisions. The main differences stem from the fact that: 1) we used a saturation model that describes the HERA data at small-x and has different energy dependence and value for the saturation scale. 2) We used a correct relation between the unintegrated gluon-density and the forward dipole-nucleon amplitude in the k_T factorization, namely Eqs. (3,4). 3) In contrast to the KLN, we kept explicitly the impact-parameter dependence of the formulation and did not assume that it is trivially factorizable as a normalization factor. 4) The relative increase of σ_s was calculated in our approach while in the KLN approach was taken from soft high-energy interactions which is alien to the saturation approach. In both approaches, lower energy data was used to fix the overall normalization factor. However, as can be seen from Figs. 3-d, 5-b, we expect that the discrepancies between our predictions and the KLN to be more pronounced at higher energies (even more in AA collisions).

In order to obtain the average transverse momentum of charge hadrons, we need also to know the value of the average fraction of energy of mini jets carried by the hadrons $\langle z\rangle$. It is seen from Fig. 4-a that an average value of $\langle z\rangle = 0.48 \div 0.5$ is remarkably able to describe the average transverse momentum of charge hadrons in a wide

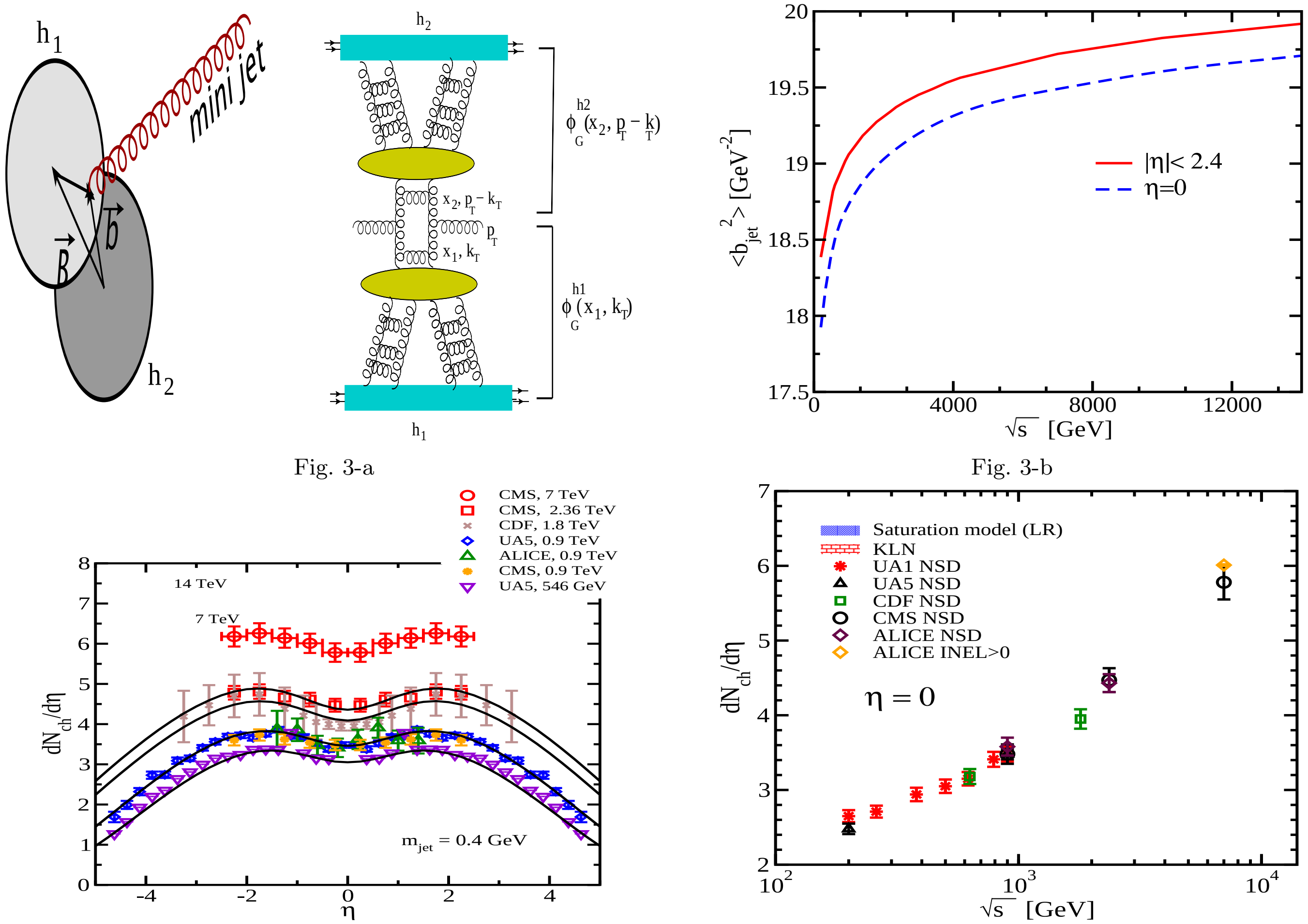

Fig. 3-a

Fig. 3-b

Fig. 3-c

Fig. 3-d

FIG. 3: a) Mini jet production in hadron-hadron collisions in the transverse plane within the k_T factorization scheme. The impact-parameter between two hadrons is $\vec{B}$. b) shows the average impact parameter of the produced mini jet $\langle b_{jet}^2 \rangle$ as a function of energy within two rapidity bins. c) The comparison with the experimental data and prediction for dN_{ch}/dy. The curves are normalized by data at $\sqrt{s} = 546\,\text{GeV}$ [5]. d) Energy dependence of the charged hadrons multiplicity in the central region of rapidity $\eta = 0$ in pp collisions. The theoretical curve (Saturation model LR) is our prediction coming from the saturation model [5]. The band indicates about 2% theoretical error. The total theoretical uncertainties is less 6% at high energies. We also show the KLN prediction [22] with the same error band as ours. Notice that in c panel we have taken a fixed mini jet mass $m_{jet} = 0.4$ GeV for all energies while in d panel uncertainties due to the assumption of a fixed energy-independent mini jet mas was included in the band. The experimental data are from Refs. [6, 18–20, 33]. The experimental error bars indicate systematic uncertainties.

range of energies. In order to further test the validity of the value $\langle z \rangle$ for the mini jets, we show in Figs. 4-b, 4-c our predictions for the differential yield of charged hadrons in the range $|\eta| < 2.4$ and at various $|\eta|$ bins for $\sqrt{s} = 2.36, 7$ and 14 TeV. The experimental data are recently reported from the CMS collaboration [6, 19]. It is seen that our predictions is in quite good agreement with experimental data at 7 TeV. We recall again that the pre-factor in Eq. (5) is the same as what we already fixed with experimental multiplicity data at low-energy $\sqrt{s} = 546$ GeV at $\eta = 0$ in Fig. 3-c. Therefore, we have no free parameters in obtaining the theoretical curves in Fig. 4. The fact that our model reasonably works at low p_T is due to the fact that the saturation scale is rather large at low p_T. In our formulation, we predicted that the differential yield of charged hadrons has a peak at low p_T. The position of the peak is approximately at $p_T \simeq m_{jet}\langle z \rangle$ [5]. The experimental data at 7 TeV shown in Figs. 4-d indeed confirmed this prediction. In the CGC scenario, the gluon saturation scale is proportional to the density of partons. The parton density is proportional to the multiplicity and, therefore, one can relate the saturation momentum in the event with the multiplicity of the hadrons n. In Fig. 4-d, we show the average transverse momentum of charged hadrons as a function of the number of charged particles for events within the kinematic range $p_T > 500$ MeV at various energies. The experimental data are from ATLAS for $\sqrt{s} = 0.9$ TeV [34]. Our prediction seems also to be in a good agreement

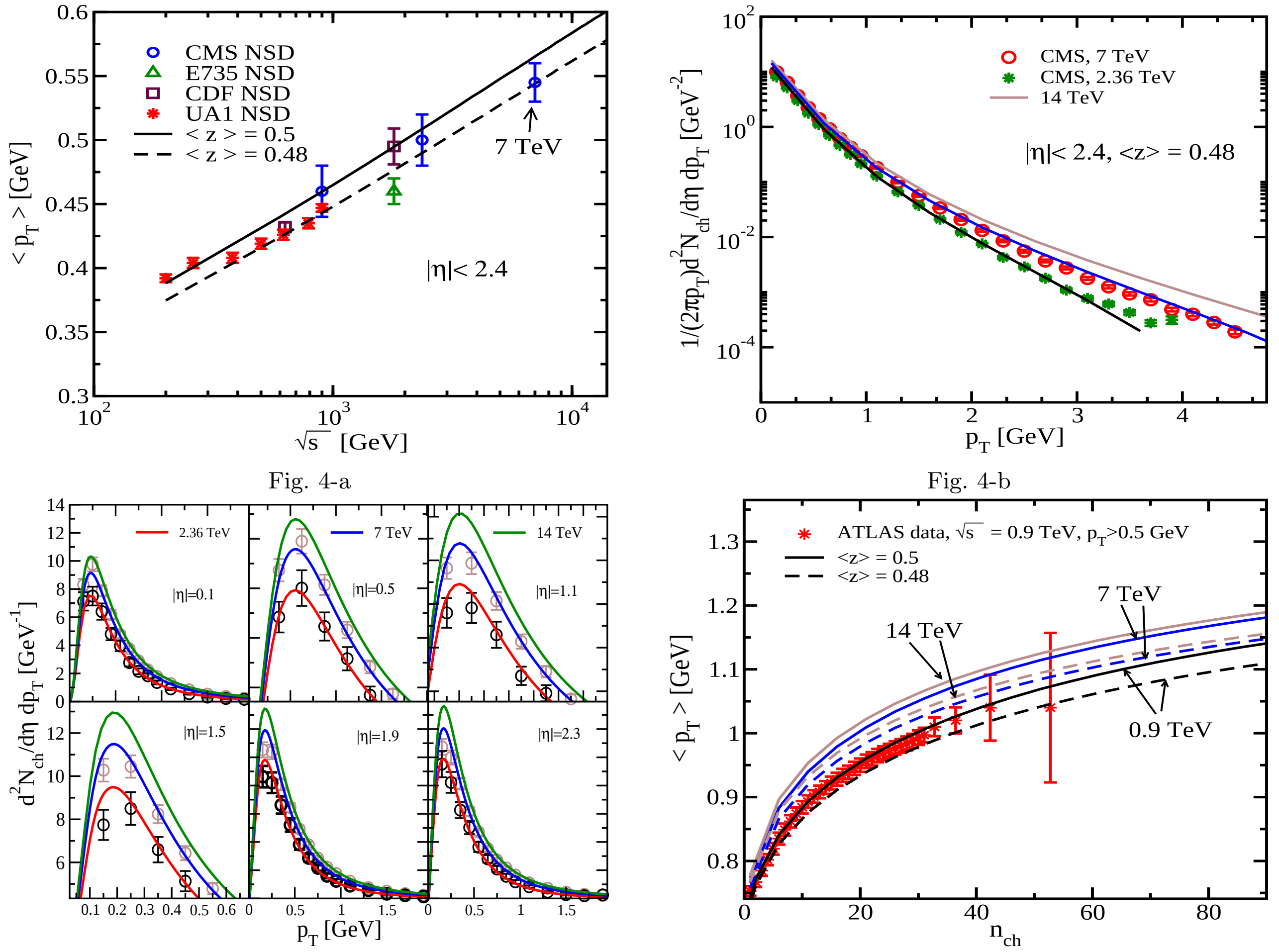

Fig. 4-a

Fig. 4-b

Fig. 4-c

Fig. 4-d

FIG. 4: a) The energy dependence of the average transverse momentum of charged hadrons. b,c)The differential yield of charged hadrons. The LHC experimental data are from the CMS collaboration [6, 19]. d) The average transverse momentum of charged hadrons as a function of the number of charged particles for events with $n_{ch} \geq 1$ within the kinematic range $p_T > 500$ MeV. The experimental data are from ATLAS for $\sqrt{s} = 0.9$ TeV and $|\eta| < 2.5$ [34]. The theoretical curves was obtained for $|\eta| = 0$ and with the same kinematic constraint $p_T > 500$ MeV at various energies for two value of $\langle z \rangle = 0.48, 0.5$ corresponding to the dashed and the solid lines, respectively. The mini jet mass is taken $m_{jet} = 0.4$ GeV in all plots. The normalization is the same as in Fig. 3.

with preliminary 7 TeV data from the ATLAS collaboration (not shown in the figure).

Finally, in Fig. 5 we show our prediction for Pb+Pb collisions at the LHC [7]. Notice that again similar to the case of *pp* collisions, we have here only two free parameters, normalization factor C and the mini jet mass which are fixed at RHIC energy $\sqrt{s} = 200$ GeV for $0 - 6\%$ centrality. Therefore, at lower/higher energies than $\sqrt{s} = 200$ GeV (for various centrality/rapidities) we do not have any free parameter. In Fig. 5-a, we show our predictions at lower RHIC energies $\sqrt{s} = 19.6$ and 130 GeV in Au-Au collisions, and also for the LHC energies $\sqrt{s} = 2.75$ and 5.5 TeV in Pb-Pb collisions for $0 - 6\%$ centrality bin. In Fig. 5-b, we show the energy dependence of $dN_{pp}/d\eta$, $dN_{AA}/d\eta$ and $(2/N_{par})dN_{AA}/d\eta$ at midrapidity $\eta = 0$ for central collisions (where N_{par} denotes the number of participant for a given centrality).

To conclude, we showed that the CGC gives very good descriptions of the first data from the LHC for the inclusive charged-hadron production in proton-proton collisions, the deep inelastic scattering at HERA at small Bjorken-x, and the hadron multiplicities in nucleus-nucleus collisions at RHIC. We believe that our predictions for nucleus-nucleus collisions at the LHC will be a crucial test of the CGC approach.

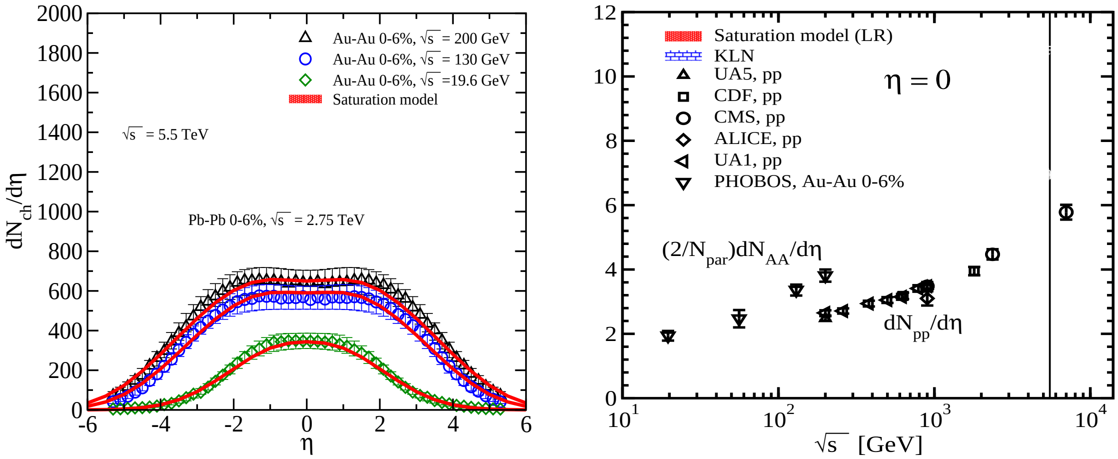

Fig. 5-a

Fig. 5-b

FIG. 5: a) Pseudo-rapidity distribution of charged particles produced in Au-Au and Pb-Pb central $0-6\%$ collisions at RHIC and the LHC energies. b) Energy dependence of the charged hadrons multiplicity at midrapidity $\eta = 0$ in central collisions in pp and AA collisions. The theoretical curve Saturation model (LR) is our prediction. The band indicates less than 3% theoretical errors. The total theoretical uncertainties is less than 7%. The experimental data are from [6, 18–20, 33, 35]. The plots are taken from Ref. [7].

IV. ACKNOWLEDGMENTS

E. L. would like to thank A. Gotsman, U. Maor and J. Miller for fruitful collaboration. This work was supported in part by Fondecyt grants 1090312 and 1100648.

[1] R. C. Brower, J. Polchinski, M. J. Strassler and C. I. Tan, JHEP **0712** (2007) 005; R. C. Brower, M. J. Strassler and C. I. Tan, JHEP **0903** (2009) 092.
[2] J. M. Maldacena, Adv. Theor. Math. Phys. **2** (1998) 231 [Int. J. Theor. Phys. **38** (1999) 1113]; S. S. Gubser, I. R. Klebanov and A. M. Polyakov, Phys. Lett. B **428** (1998) 105; E. Witten, Adv. Theor. Math. Phys. **2** (1998) 505.
[3] See for example: J. Polchinski and M. J. Strassler, JHEP **0305** (2003) 012; Phys. Rev. Lett. **88** (2002) 031601.
[4] A. V. Kotikov and L. N. Lipatov, Nucl. Phys. B **661** (2003) 19 [Erratum-ibid. B **685** (2004) 405] and references therein.
[5] E. Levin and A. H. Rezaeian, Phys. Rev. **D82** (2010) 014022 [arXiv:1005.0631].
[6] V. Khachatryan *et al.* [CMS Collaboration],Phys. Rev. Lett. **105** (2010) 022002 [arXiv:1005.3299].
[7] E. Levin and A. H. Rezaeian, Phys. Rev. **D82** (2010) 054003 [arXiv:1007.2430].
[8] R. C. Brower *et al.*, arXiv:1007.2259 ; E. Levin, I. Potashnikova, JHEP **1008** (2010) 112.
[9] M. L. Good and W. D. Walker, Phys. Rev. **120** (1960) 1857.
[10] Y. Hatta, E. Iancu and A. H. Mueller, JHEP **0801** (2008) 026.
[11] J. Bartels, J. Kotanski, A. -M. Mischler and V. Schomerus, arXiv:0912.3072.
[12] J. Bartels, M. Wusthoff, Z. Phys. **C66** (1995) 157.
[13] E. Gotsman, E. Levin, U. Maor and J. S. Miller, Eur. Phys. J. C **57** (2008) 689.
[14] M. G. Ryskin, A. D. Martin and V. A. Khoze, Eur. Phys. J. C **54** (2008) 199.
[15] S. Ostapchenko, Phys. Rev. **D81** (2010) 114028.
[16] E. Gotsman, E. Levin, U. Maor, arXiv:1010.5323.
[17] E. Gotsman, E. Levin and U. Maor, Phys. Rev. D **81** (2010) 051501.
[18] ALICE Collaboration, Eur. Phys. J. C **65** (2010) 111 [arXiv:0911.5430]; arXiv:1004.3034.
[19] CMS Collaboration, JHEP **1002** (2010) 041 [arXiv:1002.0621].
[20] S. Eidelman *et al.* [Particle Data Group Collaboration], "*Review of particle physics*", Phys. Lett. **B592** (2004) 1.
[21] L. V. Gribov, E. M. Levin and M. G. Ryskin, Phys. Rep. **100** (1983) 1; A. H. Mueller and J. Qiu, Nucl. Phys. **B268** (1986) 427; L. McLerran and R. Venugopalan, Phys. Rev. **D49** (1994) 2233; **D49** (1994) 3352; **D50**, (1994) 2225; **D53** (1996) 458; **D59** (1999) 094002; I. Balitsky, [arXiv:hep-ph/9509348]; Phys. Rev. **D60** (1999) 014020; Y. V. Kovchegov, Phys. Rev. **D60** (1999) 034008; J. Jalilian-Marian, A. Kovner, A. Leonidov and H. Weigert, Phys. Rev. **D59** (1998) 014014 ;Nucl. Phys. **B504** (1997) 415; E. Iancu, A. Leonidov and L. D. McLerran, Phys. Lett. **B510** (2001) 133; Nucl. Phys. **A692** (2001) 583; H. Weigert, Nucl. Phys. **A703** (2002) 823.
[22] D. Kharzeev, E. Levin and M. Nardi, Nucl. Phys. A **730** (2004) 448 [Erratum-ibid. A **743** (2004) 329]; Phys. Rev. C **71**

(2005) 054903; D. Kharzeev and E. Levin, Phys. Lett. B **523** (2001) 79; D. Kharzeev and M. Nardi, Phys. Lett. B **507** (2001) 121.
[23] Yu. V. Kovchegov and A. H. Mueller, Nucl. Phys. **B529** (1998) 451.
[24] Y. V. Kovchegov and K. Tuchin, Phys. Rev. D **65** (2002) 074026.
[25] M. A. Braun, Phys. Lett. **B483** (2000) 105; A. Dumitru and L. McLerran, Nucl. Phys. **A700** (2002) 492; J.P. Blaizot, F. Gelis and R. Venugopalan, Nucl. Phys. **A743** (2004) 13.
[26] G. Watt and H. Kowalski, Phys. Rev. D **78** (2008) 014016.
[27] H. Kowalski, L. Motyka and G. Watt, Phys. Rev. D **74** (2006) 074016.
[28] E. Iancu, K. Itakura and S. Munier, Phys. Lett. B **590** (2004) 199
[29] E. Levin and K. Tuchin, Nucl. Phys. B **573** (2000) 833.
[30] A. H. Rezaeian and A. Schaefer, Phys. Rev. **D81** (2010) 114032 [arXiv:0908.3695]; B. Z. Kopeliovich, E. Levin, A. H. Rezaeian and I. Schmidt, Phys. Lett. **B675** (2009) 190[arXiv:0902.4287].
[31] Y. L. Dokshitzer, V. A. Khoze and S. I. Troian, J. Phys. G **17** (1991) 1585.
[32] V. A. Khoze, W. Ochs and J. Wosiek, arXiv:hep-ph/0009298; V. A. Khoze and W. Ochs, Int. J. Mod. Phys. A **12** (1997) 2949 and reference therein.
[33] UA1 collaboration, Nucl. Phys. **B335** (1990) 261; UA5 collaboration, Z. Phys. **C33** (1986) 1; CDF collaboration, Phys. Rev. **D41** (1990) 2330; Phys. Rev. Lett. **61** (1988) 1819.
[34] ATLAS Collaboration, Phys. Lett. **B688** (2010) 21 [arXiv:1003.3124].
[35] PHOBOS collaboration, Phys. Rev. Lett. **91** (2003) 052303 [arXiv:nucl-ex/0210015].